The International Journal of Engineering and Science (IJES)
|| Volume || 13 || Issue || 4 || Pages || PP 18-33 || 2024 ||
ISSN (e): 2319 – 1813 ISSN (p): 2319 – 1805

Molecular Sieve-Based Adsorptive Denitrogenation of Air for Natural Gas and Other Applications

Emeka J. Okafor[1], America I. Efe[2], Chinedu O. Akuma[3], Egbo C. Collins[1], Success A. Philip[4], Diriyai I. Bobara[1], Chukwuemeka F. Anikpo[1], Charles N. Osia[4], Julius Esiti[5], Precious O. Ekiejareh[6], Sylvanus U. Frank[7], Samuel I. Onyeiwu[1]

[1] *Department of Petroleum and Gas Engineering, University of Port Harcourt, Nigeria*
[2]*Indorama Eleme Fertilizer & Chemicals Limited (IFL), Port Harcourt, Nigeria*
[3]*Totalsupport Limited, Port Harcourt, Nigeria*
[4]*Society of Petroleum Engineers, Port Harcourt, Nigeria*
[5]*J-Esiti Global Limited, Nigeria*
[6]*Mobil Producing Nigeria, ExxonMobil Corporation, Nigeria*
[7]*TotalEnergies Nigeria Limited*
Corresponding Author: Chinedu O. Akuma (akuma.chinedu@yahoo.com

----------ABSTRACT----------

Molecular sieve-based adsorptive denitrogenation of air for high-quality nitrogen production which can be deployed for purging, inerting, enhanced oil recovery, and other natural gas processing applications was studied by the in-situ adsorption of oxygen and the subsequent production of nitrogen. The use of both phenomenological and mathematical models for describing such operations exists, however, the influence of time optimization and cycle number on the operational performance requires further study. This work presents the pressure swing adsorption process for denitrogenation of air using 5A molecular sieves in different cycle numbers. A carbon-based process, in which the adsorbent shows preferential adsorption of oxygen over nitrogen under equilibrium conditions, is used for the production of nitrogen. This industrial air-denitrogenation unit was modeled, and the breakthrough times for both 50-second and 1000-second runs were analyzed and compared. Findings suggest that a careful adjustment of the molecular sieve properties and a good choice of isotherm properties would result in higher performance in terms of producing greater yields of purified nitrogen.

KEYWORDS;- *Pressure swing adsorption, carbon molecular sieve, nitrogen separation from air.*

Date of Submission: 02-04-2024 Date of acceptance: 13-04-2024

I. INTRODUCTION

The widespread use of nitrogen in industrial processes makes it vital for operators to understand and employ the most efficient nitrogen generation techniques. While nitrogen occurs freely in nature (constituting about 78% by volume of air), it is not readily available in its pure useful form; it is typically mixed with other component gases of air that may have an undesirable effect on industrial manufacturing processes.

Gaseous nitrogen is used in the chemical Industry as well as in the oil and gas industry for storage tank blanketing and vessel inerting applications. Commercial nitrogen is produced by a variety of air separation processes, including cryogenic liquefaction and distillation, adsorption separation, and membrane separation, but all of these methods most likely require high recompression of the methane product, which penalizes their economics[1]. All of these methods can be used to produce high-purity nitrogen for industrial use.

Cryogenic distillation is almost always the only technically and commercially feasible process solution for nitrogen removal from air as it consumes far less power per unit of air processed, requires less costly machinery, can use a relatively simple machinery configuration (based on conventional gas processing compressors), is reliable, ensures specification products even with varying feed composition and very environmentally friendly. This process involves pulling ambient air into the distillation set-up with the help of a compressor system. The compressed air is then cooled to about 10^{o}C before being passed through a series of filters to eliminate inherent moisture, oil, and other contaminants that might impede the downstream cryogenic processes.

Once the air has been cleaned, it is channeled through a heat exchanger to an expansion engine. The rapid expansion of the compressed gas within the engine will cause its temperature to fall below its condensation point (approximately -195.8 within 1 atmosphere of pressure) and liquefy. Once liquefaction is achieved, a high-purity fraction of nitrogen is distilled out of the air and channeled to storage units.

For very small Air processing plants, it may be possible to employ the mechanical methods of Pressure Swing Adsorption (PSA) or membrane technology. These processes depend on the differential speed of travel and adsorption by membranes and molecular sieves to generate nitrogen. Gas adsorption occurs when gas molecules interact with and become retained by a solid material. The reasons for this adhesion are numerous, and may include charge differences, chemical reactions, and size or shape effects **[2].** These interactions frequently differ between gas molecules, and therefore serve as a useful basis for their separation.

The fixed bed adsorption operation usually entails two major steps: an adsorption step (in which the adsorbent selectively retains the adsorbed species from the feed) and a regeneration step (the adsorbent releases the retained species, thus regenerating the adsorbent for use in the next cycle).

Specifically, the adsorption process involves the following: (a) The diffusion of a component from the bulk fluid into the pores of a solid particle; and (b) The binding of that component to the solid surface inside a pore. The driving force for the migration of the chemical species into the pore phase is the difference in concentration (Wood et al., 2018), that is, if the pore phase is poor in a component that the bulk phase is rich in, then that component will be driven to diffuse into the pores.

Figure 1.1 schematically shows how changing the pressure allows us to accomplish the regeneration, and therefore the separation. In this figure, the solid adsorbent is observed to hold more of the retained component at high pressure; therefore, when an adsorbent-containing bed is pressurized with the feed gas, the solid will be "loaded" with the adsorbed component along the line labeled "Uptake." Once the pressure is allowed to drop, the adsorbed molecules will be released along the curve labeled "Release." The curve labeled "strongly adsorbed gas isotherm" describes the maximum capacity of the solid for each pressure. The name 'isotherm' comes from the fact that this entire cycle occurs at roughly constant temperature. The "working capacity" of the adsorbent loading is defined as the difference between the isotherm point at P_{low} and the isotherm point at P_{High} in the figure. Since the y-axis is 'loading', given by (mass adsorbed component)/(mass adsorbent), the difference represents the maximum mass of the adsorbed gas that can be recovered, per cycle, per mass of adsorbent.

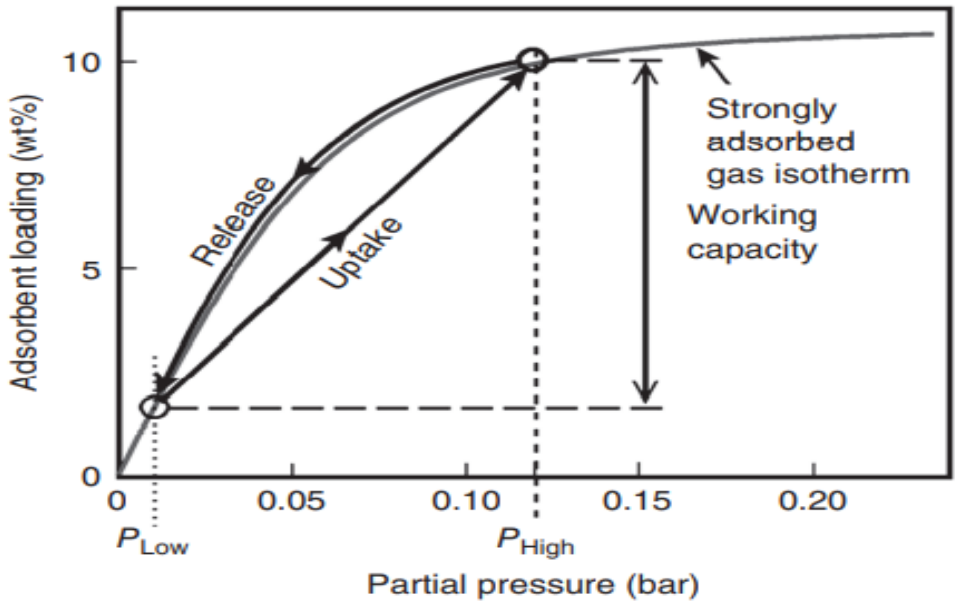

Figure 1.1: The basic schematic isotherms in a PSA operation for an adsorption process [2]

Three (3) common types of adsorbents are usually employed in the industry. They are Alumina, silica gel, and Molecular sieves. Alumina produces an excellent dew point depression value as low as -100ºF but requires much more heat for regeneration. Its tendency to adsorb heavy hydrocarbons is high, and it is difficult to remove these during regeneration. Silica Gels can dehydrate gas to as low as 10 ppm and have the greatest ease of regeneration of all desiccants. They adsorb heavy hydrocarbons but release them relatively more easily during regeneration. Molecular sieves have been widely used to purify natural gas and air in the past 50 years;

most times it stands as the only solution for LNG and NGL recovery. They are the basic building blocks for various zeolite structures, such as zeolites Å and X, the most common commercial adsorbents.

Successive adsorption and desorption cycles affect the bed capacity. The efficiency of adsorbent beds decreases as the number of operating cycles increases [3].

Prediction of adsorption vessel dynamics requires a simultaneous solution of a set of coupled partial differential equations (PDE) representing material, energy, and moment balances under appropriate boundary conditions [4]. Fixed bed adsorption models include an equation for the adsorption isotherm, equations for mass and energy balance in the gas phase, and equations for mass and energy balance within the particle [5]. Many approaches to describe the adsorption process can be found in the literature, differing on the approximations made in the modeling of equilibrium and transport equations. [6] developed a mathematical model for the multicomponent adsorption process in molecular sieve bed type 5A. They concluded that the breakthrough time reduces linearly with the square of the particle diameter. [7] evaluated the effect of process parameters (pressure, temperature, and feed composition) in the dehydration of natural gas in molecular sieve type 4A. The results showed that the lower the adsorption pressure and temperature, the faster the equilibrium is reached.

The objective of this work is to model the operation of an Air-denitrogenation unit employing molecular sieves type 5A installed in a typical Nitrogen-production platform. This work comprises (a) Summarized discussions of adsorption equilibrium and the theoretical assumptions behind the various mathematical models that have been used to describe it, (b) the assessment of the adsorption isotherm model that describes the experimental adsorption data found in the literature more adequately, (c) the simulation of experimental data from the literature using in Aspen Adsorption simulator tool, to verify the adequacy of the model hypotheses, and (d) the modeling of field operational data, with an assessment of the effect of cycle duration on the bed performance.

II. MATERIALS AND METHODS

To simulate the air denitrogenation, a reduced binary system comprising only nitrogen (N_2) and oxygen (O_2) was chosen. Thermodynamic properties and Vapor-Liquid Equilibrium (VLE) are calculated via the Peng-Robinson Equation of State (PR-EOS).

The influence of other factional air components such as CO_2 and water vapor on the adsorption was neglected because (a) N_2 and O_2 account for more than 98% of air composition and (b) the calibration of the adsorption model is a critical step; it is difficult to find reliable equilibrium Molecular sieve adsorption data for the smaller fractional components.

Simulation parameters include gas composition, temperature, pressure, adsorption bed properties, and the adsorption equilibrium model, which is expressed as a set of adsorption isotherms with their characteristic parameters.

Two simulation environments were employed: (a) Aspen Plus (Aspen Technology, Inc.) using PR-EOS with binary interaction parameters (BIPs) from the Aspen Plus library to determine the composition and thermodynamic properties of the Air feed and (b) ADSIM (Aspen Technology, Inc.) to dynamically simulate PSA-MS phases: adsorption and bed regeneration.

In addition, Microsoft Excel (Microsoft Corporation) was used for estimating isotherm parameters by fitting adsorption isotherms onto adsorption equilibrium data from the literature for pure N_2 and O_2 with Molecular sieve 5 Å Zeolite.

ASPEN data block formulation

The specified data for the process. simulation model as earlier stated was conducted utilizing the ADSIM library of the Aspen Adsorption software. Each of the blocks was duly specified with the required data for a smooth running of the model.

Tables 2.1 below illustrate an inlet flow rate of about 3.3e-6 kmols for the air binary components with Nitrogen having a higher composition of 0.79 kmol/kmol while Oxygen occupies the remaining 0.21 kmol/kmol. An isothermal condition of 298.15-degree kelvin was used throughout the process and the inlet pressure was set at 3.045bar. Table 2.2 comprises the carbon molecular sieve (CMS) specifications and the adsorption beds parameters. Bed layer initial conditions are indicated in Table 2.3, and Tables 2.4 and 2.5 show the initial data arrangements for the Nitrogen product and Oxygen desorption initial setup conditions respectively. Preferences were given to Nitrogen in the formal and to Oxygen in the latter table with considerations to the expected volumetric yields at each of these nodes.

Table 2.1: The Nitrogen and Oxygen Feed Composition

AIR-FEED DATA				
	Value	Units	Spec	Description
F	3.2704e-006	kmol/s	Free	Flowrate
Y_Fwd(*)				
Y_Fwd("N2")	0.79	kmol/kmol	Fixed	Composition in forward direction
Y_Fwd("O2")	0.21	kmol/kmol	Fixed	Composition in forward direction
T_Fwd	298.15	K	Fixed	Temperature in forward direction
P	3.045	bar	Fixed	Boundary pressure

Table 2.2: Adsorption Bed Layer Data

Adsorption Bed CMS Data			
	Value	Units	Description
Hb	0.35	m	Height of adsorbent layer
Db	0.035	m	Internal diameter of adsorbent layer
Ei	0.4	m3 void/m3 bed	Inter-particle voidage
Ep	0.0	m3 void/m3 bead	Intra-particle voidage
RHOs	592.0	kg/m3	Bulk solid density of adsorbent
Rp	1.05	mm	Adsorbent particle radius
SFac	1.0	n/a	Adsorbent shape factor
MTC(*)			
MTC("N2")	0.007605	1/s	Constant mass transfer coefficients
MTC("O2")	0.04476	1/s	Constant mass transfer coefficients
IP(*)			
IP(1,"N2")	0.0090108	n/a	Isotherm parameter
IP(1,"O2")	0.0093653	n/a	Isotherm parameter
IP(2,"N2")	3.3712	n/a	Isotherm parameter
IP(2,"O2")	3.5038	n/a	Isotherm parameter
Direction	0.0	n/a	Specified flow direction (self determined: 0, forward: 1)

Table 2.3: Bed Layer Initial Data

Bed Layer Initial Data					
	Value	Units	Spec	Derivative	Description
ProfileType	Constant				Is the bed initially specified with constant or linearly varying conditions
Y_First_Node(*)					
Y_First_Node("N2")	1.0	kmol/kmol	Initial		Mole fraction within first element
Y_First_Node("O2")	0.0	kmol/kmol	Initial		Mole fraction within first element
Vg_First_Node	3.55e-004	m/s	Initial		Gas velocity within first element
W_First_Node(*)					
W_First_Node("N2")	0.0	kmol/kg	RateInitial	0.0	Solid loading within first element
W_First_Node("O2")	0.0	kmol/kg	RateInitial	0.0	Solid loading within first element

Table 2.4: The Light Product Block Data

Product Block Data				
	Value	Units	Spec	Description
F	2.8823e-006	kmol/s	Free	Flowrate
Y_Rev(*)				
Y_Rev("N2")	0.9	kmol/kmol	Fixed	Composition in reverse direction
Y_Rev("O2")	0.1	kmol/kmol	Fixed	Composition in reverse direction
T_Rev	298.15	K	Fixed	Temperature in reverse direction
P	3.0	bar	Fixed	Boundary pressure

Table 2.5: The Heavy Product (Waste) Block Data

Waste Block Data				
	Value	Units	Spec	Description
F	3.4560.e-007	kmol/s	Free	Flowrate
Y_Rev(*)				
Y_Rev("N2")	0.1	kmol/kmol	Fixed	Composition in reverse direction
Y_Rev("O2")	0.9	kmol/kmol	Fixed	Composition in reverse direction
T_Rev	298.15	K	Fixed	Temperature in reverse direction
P	1.0	bar	Fixed	Boundary pressure

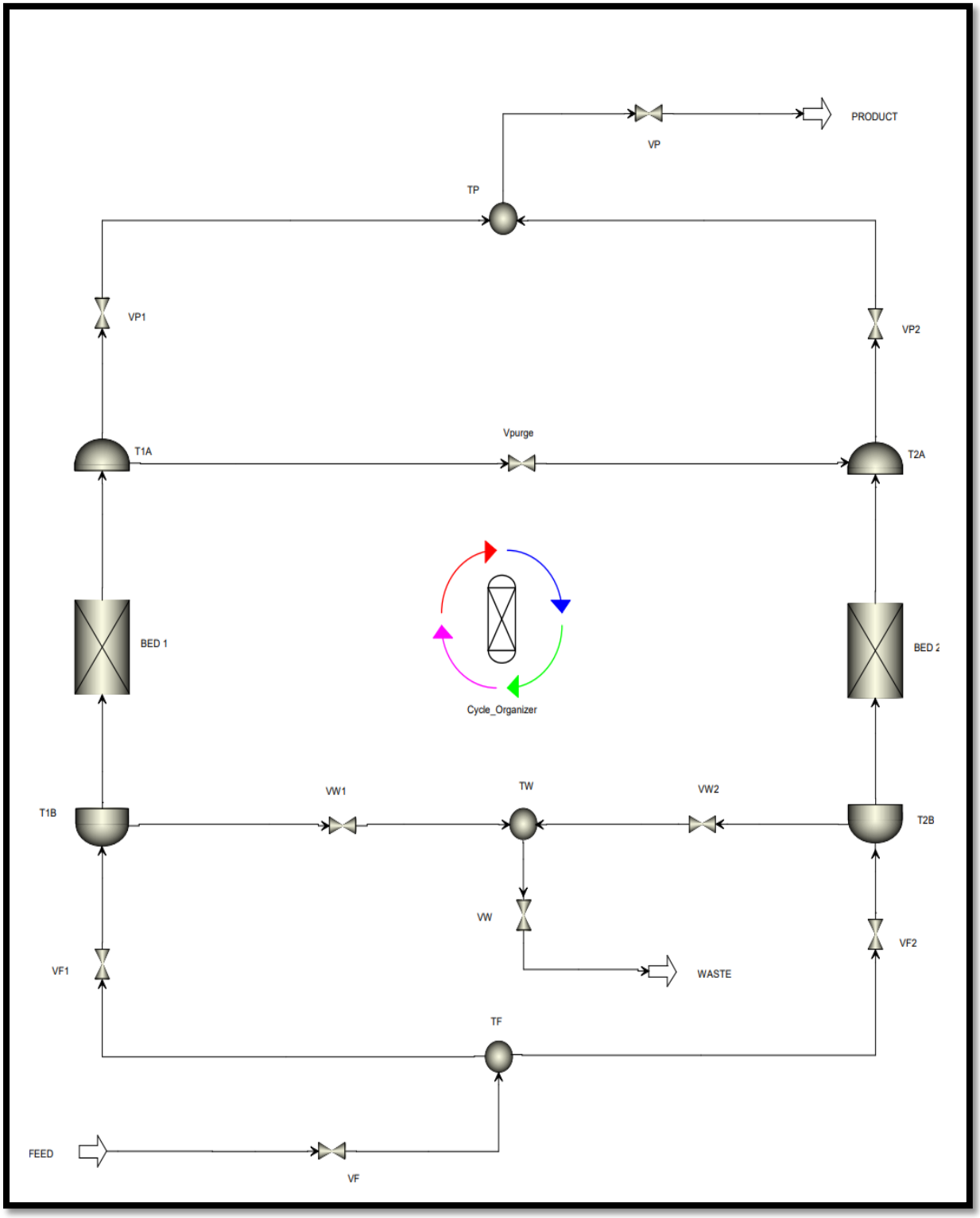

Figure 2.1: ADSIM Model Flow Diagram [2]

Figure 2.1 above shows the cyclic PSA model built with two beds for the binary separation. The process is cyclic because the beds will alternate between adsorption and desorption. While Bed 1 is in the adsorption phase, Bed 2 is in the desorption (regeneration) phase. During the adsorption stage, at a relatively high pressure, the solid adsorbent in the bed will selectively adsorb the oxygen from the binary gas mixture. The leftover nitrogen produced in this step is referred to as the raffinate or the light product (LP) since it has been refined by having the oxygen removed. In the following desorption step, by lowering the gas-phase partial pressure inside the bed, the adsorbent releases the adsorbed components, in this case oxygen; to produce a gas

stream called the extract (because it was extracted from the main gas stream.) It is also referred to as the heavy product (HP) because it is enriched in the more strongly adsorbed components; in this case, it was termed as the waste product. The above-described cycle repeats afterward.

ASSESSMENT OF EQUILIBRIUM MODEL AND ADSORPTION ISOTHERM

The assessment based on calibrated adsorption isotherms for the two gas species, the performance of adsorption denitrogenation of air can be evaluated in a PSA-MS unit in terms of (a) adsorbent capacity at the temperature and pressure of operation; (b) bed regeneration time and the necessary variation of pressure (PSA); and (c) size of the unused bed, therefore determining the correct design of the adsorption bed [5]. A typical adsorption isotherm for microporous adsorbents – i.e., adsorbents whose pore size does not differ much from the molecular diameter [8] – can be classically described by the Extended Langmuir I model as shown in Eq. 2.1 and 2.2 below [2], where a_i (i = 1, …8) are the adjustable parameters of isotherms and q_i (kmol/kg) is the adsorbed quantity of component i in equilibrium. The equations can be understood as the dynamic equilibrium expression of a well-known chemical reaction analog between gaseous molecules (A) and the free active sites (B) of adsorbent-producing adsorbed molecules on active sites (AB): A(g) + B(s) ↔ AB(s).

$$q_i = \frac{a_i c_i}{1 + \sum_{j=1}^{NC} b_j c_j} \qquad \text{Eqn. 2.1}$$

$$q_i = \frac{a_i c_i}{1 + \sum_{j=1}^{NC} b_j c_j} + \frac{\alpha_i c_i}{1 + \sum_{j=1}^{NC} \beta_j c_j} \qquad \text{Eqn. 2.2}$$

Equation 2.1 and 2.2: the Extended Langmuir 1 isotherm model [2]

The Extended Langmuir 1 model was used as the assumed isotherm for the gas bed layers since this isotherm is a function of either partial pressure or concentration. It is relatively simple and reasonably accurate in estimating multi-component adsorption behavior. They work well for binary mixtures. Accuracy of extended Langmuir isotherm, however, decreases as the pressure increases.

In order to control the various stages in the model, an ADSIM Cycle Organizer package was utilized. The Cycle Organizer enabled specific and automatic calls to duty of the seven valves that directly interface with the two-bed layers in the model operations. The sequential valve schedule for the two-bed, four-step process and the valve specification/position definition are as shown in Figure 2.2, table 2.6, and Table 2.7 and described in Table 2.8 below.

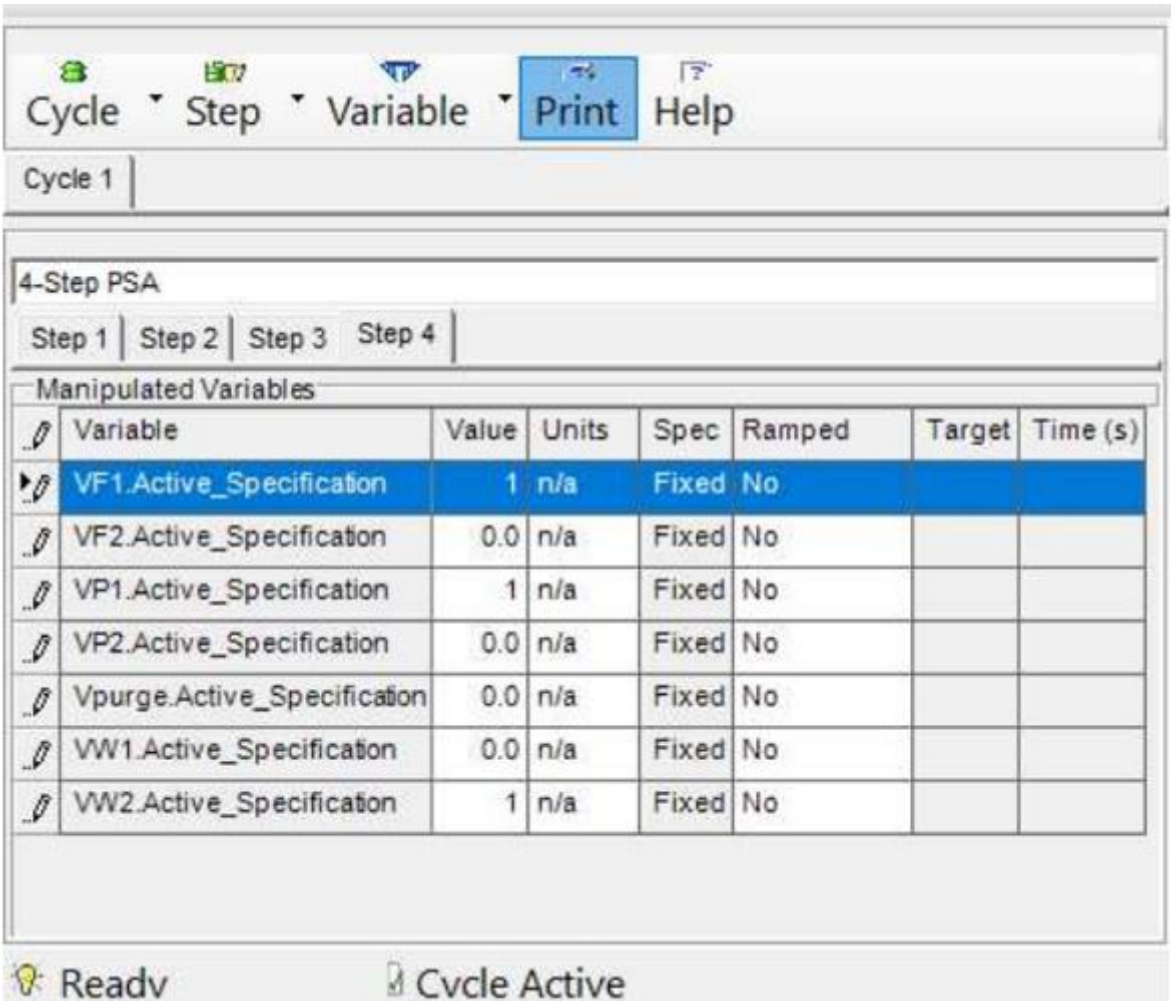

Figure 2.2: Cycle Organizer Specification[2]

Table 2.6: The sequential valve schedule for a two-bed, four-step process[2]

Steps	Function	VF1	VF2	VW1	VW2	VP1	VP2	VPurge
1	Adsorb Bed 1, Purge Bed 2	1	0	0	1	1	0	2
2	Blow Down Bed 1, Pressurize Bed 2	0	1	1	0	0	1	0
3	Purge Bed 1, Adsorb Bed 2	0	1	1	0	0	1	2
4	Pressurize Bed 1, Blow Down Bed 2	1	0	0	1	1	0	0

Table 2.7: Valve specification/position meanings

Valves Specifications Meanings	
0	The valve is fully closed (the flow rate through the valve always be zero)
1	The valve is fully open (the flow rate through the valve will be determined by mass balance)
2	The valve's flow rate will have a linear relationship with pressure drop
3	The valve will have a fixed flow rate

Table 2.8: The PSA steps description

Step Name	Description	Motivation
Pressurization	In this step, the bed is pressurized, typically with material from the feed stream	This step forces any enriched gas still present in the bed toward the product stream, while raising the bed pressure in preparation for the adsorption step
Adsorption	This step is operated at high pressure; the gas and solid interact to extract the strongly adsorbed component. The raffinate is collected during this step, and its withdrawal may or may not lower the bed pressure	Allow maximum extract adsorption and recovery of the less-adsorbed component
Blow-down	One end of the bed is connected to a low-pressure sink. If the blowdown is counter-current, the raffinate will have higher purity. Co-current blowdown is sometimes used to improve extract purity (see also: equilibration)	Purge the bed of the remaining raffinate gas and prepare the bed for low pressure desorption
Regeneration	The solid phase is allowed to release the adsorbed component, and the gas is collected as the extract. May be done as in vacuum, and with or without a purge	Regenerate the solid for the next Adsorption cycle. The use of a purge may involve a trade-off between the extract purity and raffinate recovery
Equilibration/ equalization	The high-pressure bed is connected to the low-pressure bed, typically at the raffinate end	Lower energy consumption (less pressurization required)

III. RESULTS AND DISCUSSION

In this PSA system, the zeolite preferentially adsorbs O_2 at higher pressure in the adsorption step and releases O_2 when the pressure drops during the desorption step. Part of the raffinate/light pressure (LP) gas passes through the Purge Valve at controlled pressure to offset the pressure drop required for the PSA regeneration or desorption phase. Note that the Purge Valve is set as a reversible flow setter just like every other valve in this process modeling and hence can interface between bed 1 and bed 2 as instructed by the Cycle Organizer that is set at 40s intervals.

After the model had been duly specified, the flow sheet was initialized and ran for 10 cycles at 50 seconds and 1000 seconds respectively. Below are the various results from the blocks of interest.

The product composition plot and history table above show the Nitrogen (LP) and Oxygen (HP) compositions as collected from the product end of the model. The breakthrough curve looks normal while the O_2 gets adsorbed initially in the CMS bed layer resulting in a higher fraction of H2 in the product stream. However, the bed eventually becomes saturated, and the yield matches the feed. The cycle repeats severally yielding the light and heavy products at the product and waste blocks.

Figure 4.1, Table 4.1, and Figure 4.2, Table 4.2 shows the adsorption of O_2 and release of N_2 as the product. Figure 4.1, and Table 4.1 clearly show these changes as the first cycle completes in the preset 40 seconds interval.

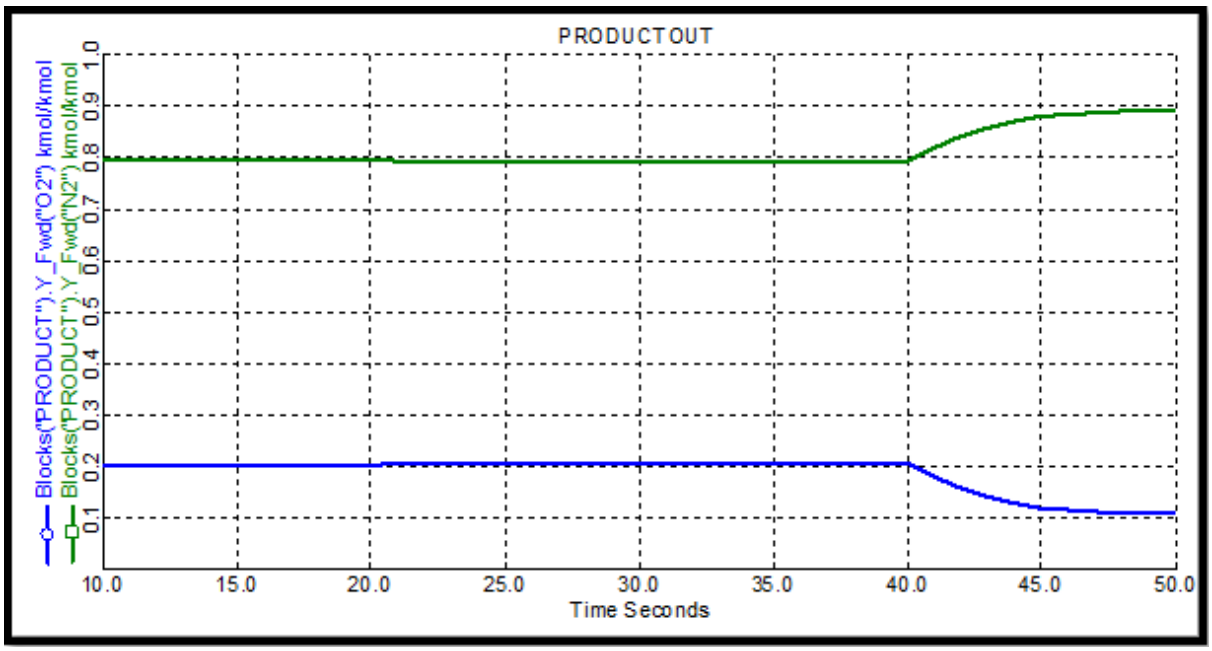

Figure 4.1: Product Composition Plot at 50s

Table 4.1: Product Outcome Composition History at 50s

Product History Table at 50 Seconds		
Time	Blocks("PRODUCT").Y_Fwd("O2")	Blocks("PRODUCT").Y_Fwd("N2")
Seconds	kmol/kmol	kmol/kmol
0.0	0.109328	0.890672
1.0	0.15225	0.84775
2.0	0.178563	0.821437
3.0	0.190608	0.809392
4.0	0.195649	0.804351
5.0	0.197914	0.802086
6.0	0.199561	0.800439
7.0	0.200264	0.799736
8.0	0.200967	0.799033
9.0	0.201485	0.798515
10.0	0.201873	0.798127
11.0	0.202261	0.797739
12.0	0.202649	0.797351
13.0	0.20296	0.79704
14.0	0.203244	0.796756
15.0	0.203528	0.796472

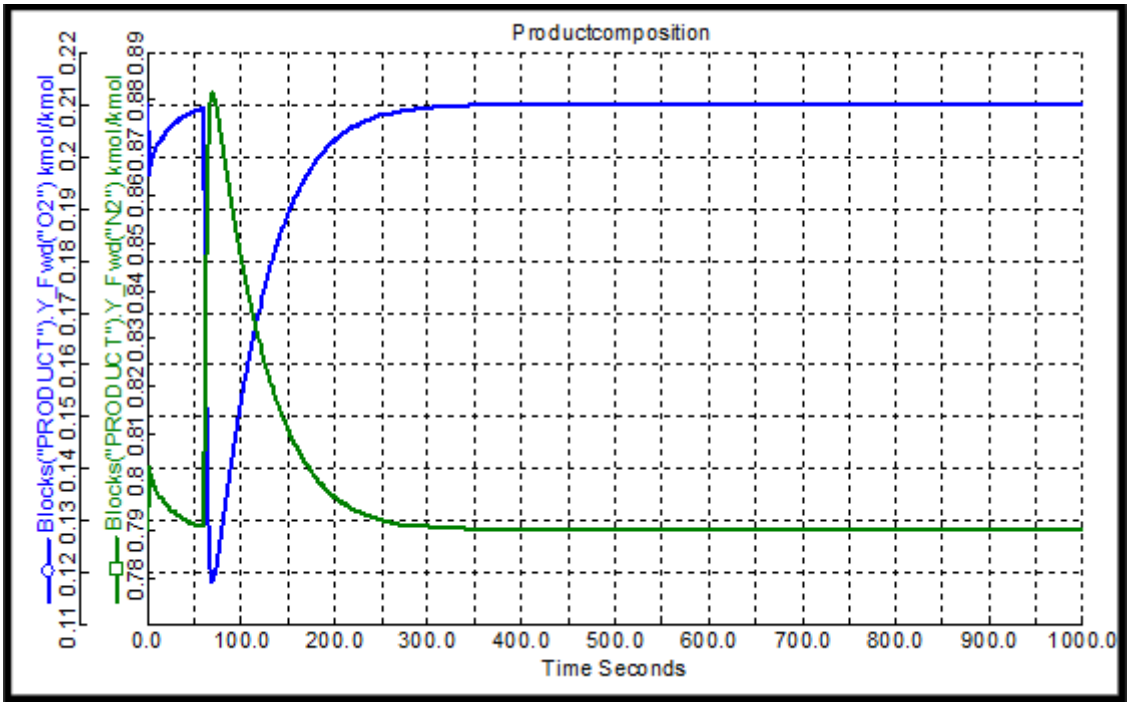

Figure 4.2: Product Composition Plot at 1000s

Table 4.2: Product Outcome Composition History at 1000s

Product History Table at 1000 Seconds		
Time	Blocks("PRODUCT").Y_Fwd("O2")	Blocks("PRODUCT").Y_Fwd("N2")
Seconds	kmol/kmol	kmol/kmol
0.0	0.210011	0.789989
1.0	0.196775	0.803225
2.0	0.197395	0.802605
3.0	0.198584	0.801416
4.0	0.199367	0.800633
5.0	0.199939	0.800061
6.0	0.200459	0.799541
7.0	0.200875	0.799125
8.0	0.201291	0.798709
9.0	0.201667	0.798333
10.0	0.202008	0.797992
11.0	0.202349	0.797651
12.0	0.20269	0.79731
13.0	0.20299	0.79701
14.0	0.203267	0.796733
15.0	0.203544	0.796456

Figure 4.3, Table 4.3, and Figure 4.4, Table 4.4 shows the desorption of O_2 in the waste outlet. The 50-second simulation can be seen to converge at 40 seconds cycle, indicating that more O_2 component is released at this end than the N_2 component.

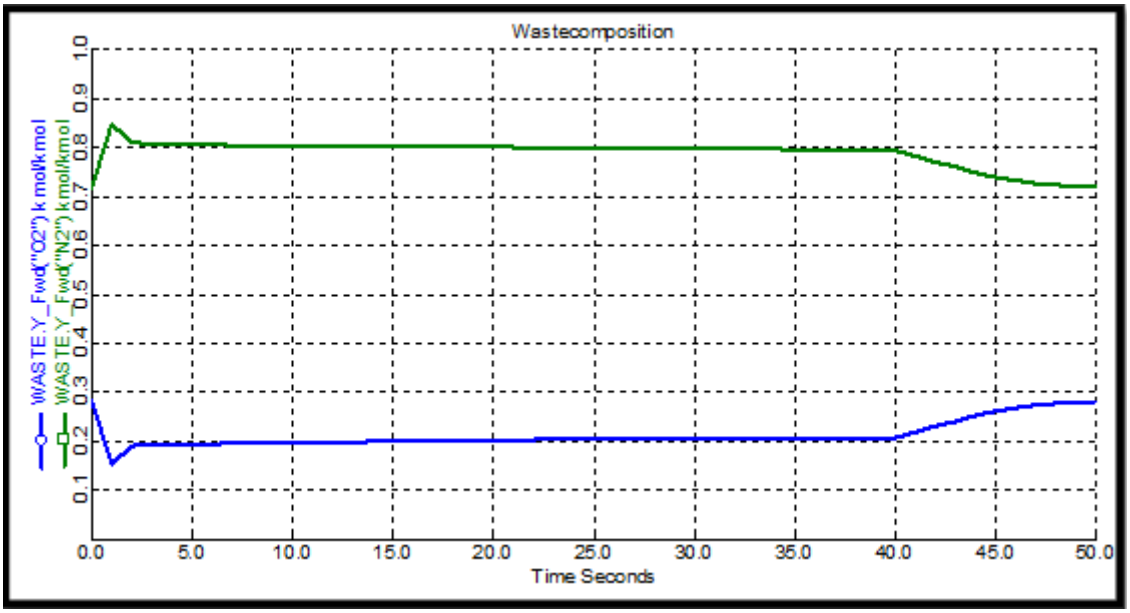

Figure 4.3: Product Waste or HP Composition Plot at 50s

Table 4.3: Product Waste Composition History at 50s

Waste Composition History Table for 50s		
Time	WASTE.Y_Fwd("O2")	WASTE.Y_Fwd("N2")
Seconds	kmol/kmol	kmol/kmol
0.0	0.282218	0.717782
1.0	0.152322	0.847678
2.0	0.189324	0.810676
3.0	0.192928	0.807072
4.0	0.193761	0.806239
5.0	0.194408	0.805592
6.0	0.195016	0.804984
7.0	0.195567	0.804433
8.0	0.196118	0.803882
9.0	0.196624	0.803376
10.0	0.197097	0.802903
11.0	0.19757	0.80243
12.0	0.198044	0.801956
13.0	0.198456	0.801544
14.0	0.198847	0.801153
15.0	0.199237	0.800763

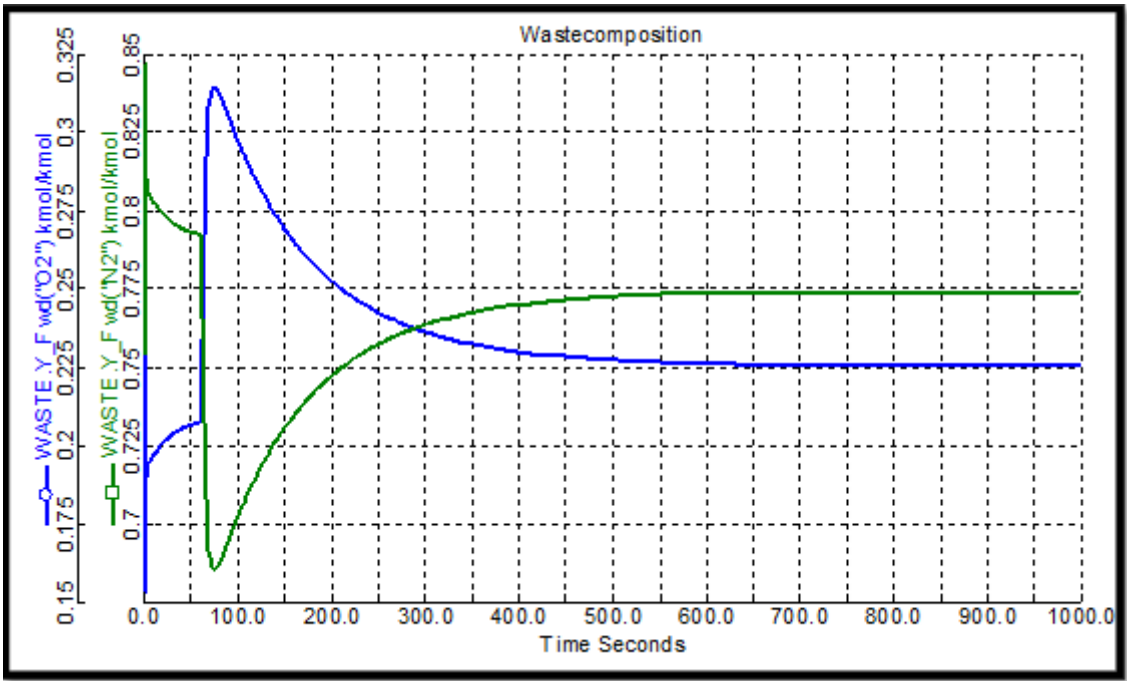

Figure 4.4: Product Waste or HP Composition Plot at 1000s

Table 4.4: Product Waste Composition History at 1000s

Waste Composition History Table for 1000s		
Time	WASTE.Y_Fwd("O2")	WASTE.Y_Fwd("N2")
Seconds	kmol/kmol	kmol/kmol
0.0	0.245525	0.754475
1.0	0.153102	0.846898
2.0	0.189368	0.810632
3.0	0.192926	0.807074
4.0	0.193759	0.806241
5.0	0.194408	0.805592
6.0	0.195017	0.804983
7.0	0.195567	0.804433
8.0	0.196117	0.803883
9.0	0.196625	0.803375
10.0	0.197097	0.802903
11.0	0.197568	0.802432
12.0	0.19804	0.80196
13.0	0.198458	0.801542
14.0	0.198848	0.801152
15.0	0.199237	0.800763

Figure 4.5, Table 4.5, and Figure 4.6, Table 4.6 show the N_2 and O_2 molar components at the outlet point of the Bed layer after adsorption. The breakout point occurred at the eleventh node at X=1.04 and Y=0.287 in Figure 4.5.

Examining the Bed Layer composition plot, we see that we achieved about 0.95 kmol/kmol purified Nitrogen concentration and about 0.05 kmol/kmol fractional composition of Oxygen after the breakout.

A careful adjustment of the molecular sieve properties or choice and isotherm properties will yield greater purified Nitrogen composition.

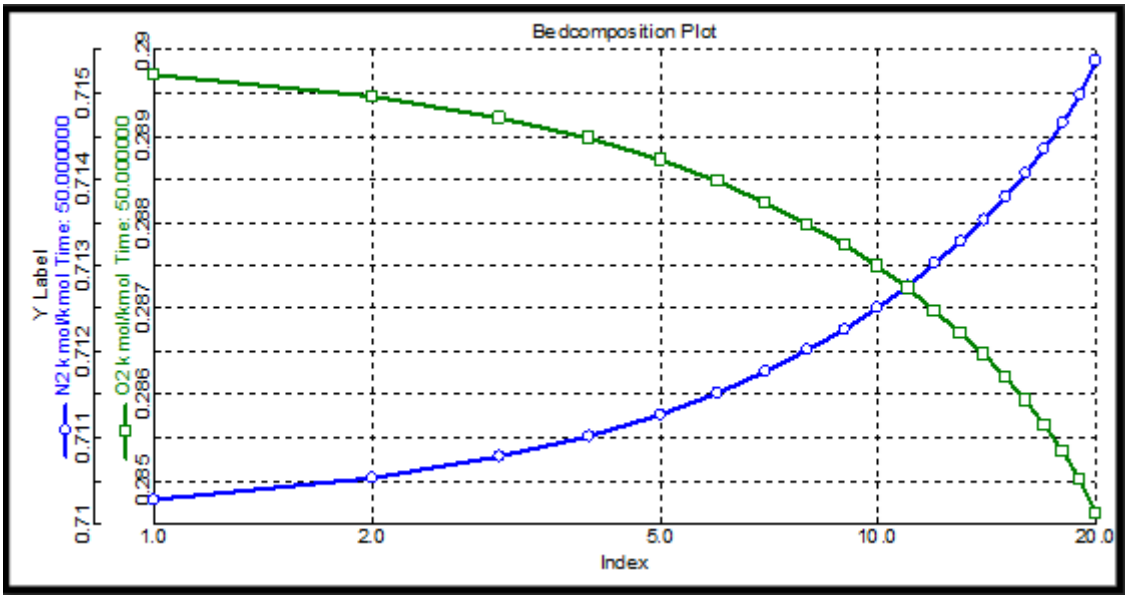

Figure 4.5: The Axial or Bed Layer Composition Plot at 50s

Table 4.5: Bed Layer Composition History at 50s

Bed Layer Composition History											
Time											
Seconds		1	2	3	4	5	6	7	8	9	10
0.0	N2	1.0	1.0	1.0	1.0	1.0	1.0	1.0	1.0	1.0	1.0
	O2	0.0	0.0	0.0	0.0	0.0	0.0	0.0	0.0	0.0	0.0
1.0	N2	0.790832	0.792033	0.793233	0.794434	0.795636	0.796838	0.79804	0.799243	0.800446	0.80165
	O2	0.209168	0.207967	0.206767	0.205566	0.204364	0.203162	0.20196	0.200757	0.199554	0.19835
2.0	N2	0.790548	0.791105	0.791667	0.792235	0.792807	0.793385	0.793967	0.794554	0.795146	0.795743
	O2	0.209452	0.208895	0.208333	0.207765	0.207193	0.206615	0.206033	0.205446	0.204854	0.204257
3.0	N2	0.790526	0.791055	0.791576	0.792101	0.792626	0.793151	0.793676	0.794201	0.794726	0.795251
	O2	0.209474	0.208949	0.208424	0.207899	0.207374	0.206849	0.206324	0.205799	0.205274	0.204749
4.0	N2	0.790505	0.791004	0.791508	0.792011	0.792513	0.79301	0.793511	0.794012	0.794512	0.795013
	O2	0.209496	0.208996	0.208494	0.207992	0.207491	0.20699	0.206489	0.205988	0.205488	0.204987
5.0	N2	0.790484	0.790962	0.79144	0.79192	0.792399	0.79288	0.79336	0.793839	0.794318	0.794797
	O2	0.209517	0.209039	0.208559	0.20808	0.207601	0.207121	0.206642	0.206163	0.205685	0.205206
6.0	N2	0.790462	0.79092	0.791379	0.791838	0.792293	0.792751	0.793209	0.793667	0.794124	0.794582
	O2	0.209539	0.209082	0.208624	0.208165	0.207707	0.207249	0.206791	0.206333	0.205876	0.205418
7.0	N2	0.790441	0.790879	0.791318	0.791757	0.792196	0.792634	0.793073	0.793512	0.79395	0.794388
	O2	0.209561	0.209121	0.208682	0.208243	0.207804	0.207366	0.206927	0.206488	0.20605	0.205612
8.0	N2	0.79042	0.790841	0.791262	0.791682	0.792098	0.792518	0.792937	0.793357	0.793776	0.794195
	O2	0.209579	0.20916	0.208741	0.208321	0.207902	0.207482	0.207063	0.206643	0.206224	0.205805
9.0	N2	0.790403	0.790804	0.791206	0.791608	0.792012	0.792415	0.792813	0.793215	0.793616	0.794018
	O2	0.209598	0.209196	0.208794	0.208392	0.20799	0.207589	0.207187	0.206785	0.206384	0.205982
10.0	N2	0.790387	0.790772	0.791158	0.791541	0.791926	0.792312	0.792697	0.793082	0.793467	0.793852

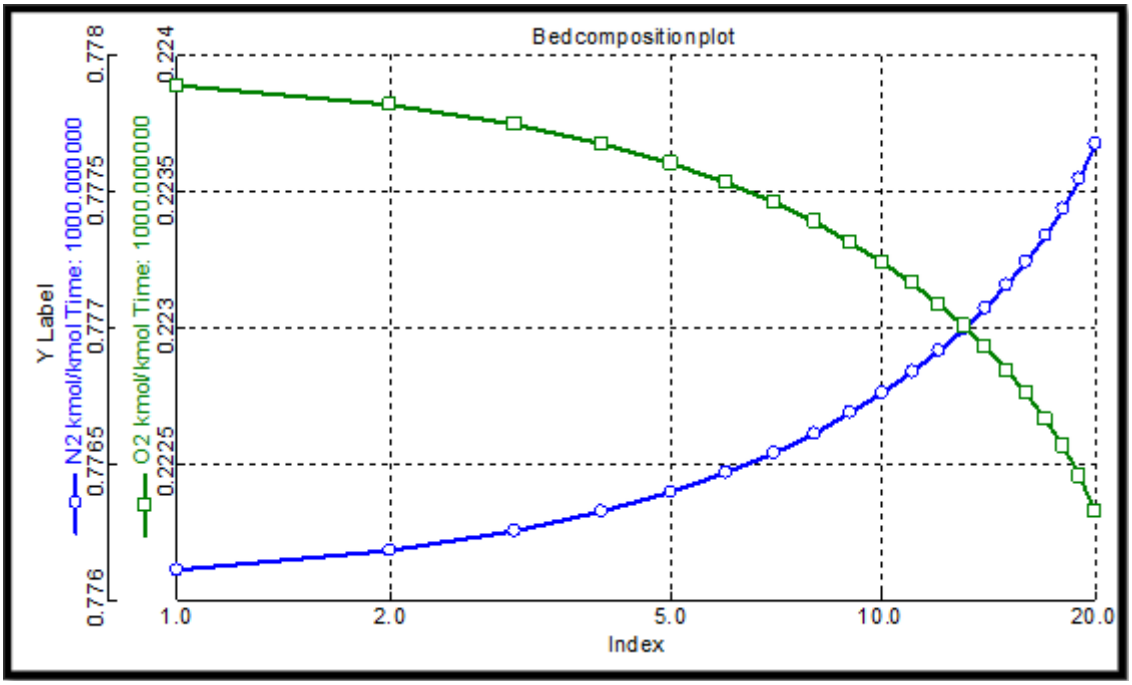

Figure 4.6: The Axial or Bed Layer Composition Plot at 1000s

Table 4.6: Bed Layer Composition History at 1000s

Bed Layer Composition History											
Time											
Sec.		1	2	3	4	5	6	7	8	9	10
0.0	N2	1.0	1.0	1.0	1.0	1.0	1.0	1.0	1.0	1.0	1.0
	O2	0.0	0.0	0.0	0.0	0.0	0.0	0.0	0.0	0.0	0.0
1.0	N2	0.791034	0.792233	0.793433	0.794633	0.795834	0.797035	0.798236	0.799438	0.80064	0.801842
	O2	0.208966	0.207767	0.206567	0.205367	0.204166	0.202965	0.201764	0.200562	0.19936	0.198158
2.0	N2	0.790552	0.791111	0.791675	0.792244	0.792818	0.793398	0.793981	0.79457	0.795164	0.795762
	O2	0.209448	0.208889	0.208325	0.207756	0.207182	0.206602	0.206019	0.20543	0.204836	0.204238
3.0	N2	0.790528	0.791051	0.791576	0.792102	0.792627	0.793152	0.793677	0.794202	0.794727	0.795253
	O2	0.209474	0.208949	0.208424	0.207898	0.207373	0.206848	0.206323	0.205798	0.205273	0.204747
4.0	N2	0.790504	0.791007	0.791508	0.792011	0.792509	0.79301	0.793511	0.794012	0.794513	0.795013
	O2	0.209497	0.208996	0.208494	0.207992	0.207491	0.20699	0.206489	0.205988	0.205487	0.204987
5.0	N2	0.79048	0.790962	0.79144	0.79192	0.792401	0.792881	0.79336	0.793839	0.794319	0.794797
	O2	0.20952	0.209039	0.208559	0.20808	0.2076	0.207121	0.206642	0.206163	0.205684	0.205206
6.0	N2	0.790461	0.790918	0.791379	0.791838	0.792293	0.792751	0.793209	0.793667	0.794124	0.794582
	O2	0.20954	0.209082	0.208624	0.208165	0.207707	0.207249	0.206791	0.206333	0.205876	0.205418
7.0	N2	0.790441	0.79088	0.791318	0.791757	0.792198	0.792635	0.793073	0.793512	0.79395	0.794389
	O2	0.209561	0.209121	0.208682	0.208243	0.207804	0.207365	0.206927	0.206488	0.20605	0.205611
8.0	N2	0.790422	0.790842	0.791262	0.791682	0.792104	0.792518	0.792938	0.793357	0.793777	0.794196
	O2	0.209579	0.20916	0.20874	0.208321	0.207901	0.207482	0.207062	0.206643	0.206223	0.205804
9.0	N2	0.790402	0.790804	0.791206	0.791608	0.792009	0.792415	0.792813	0.793215	0.793616	0.794018
	O2	0.209598	0.209196	0.208794	0.208392	0.207991	0.207589	0.207187	0.206785	0.206384	0.205982
10.0	N2	0.790386	0.790772	0.791158	0.791543	0.791927	0.792312	0.792697	0.793082	0.793468	0.793853

IV. CONCLUSION

Among the isotherm models evaluated, the Extended Langmuir 1 was the one that best adjusted the experimental data for the two major air components (N_2 and O_2) analyzed in this study. This adsorption model was able to satisfactorily predict the results of the breakthrough time of experimental data. The analysis of the effect of cycle number and time optimization on the operation performance shows that a careful adjustment of the molecular sieve properties and or a good choice of isotherm properties will yield greater purified Nitrogen composition. The varying outlet composition could be caused by adsorbent contamination, failures in the regeneration process, and damage to the adsorbent structure in the regeneration process, among other reasons. These results show that care must be exercised when trying to optimize the cycle process of any adsorption process.

REFERENCE

[1] J.C. Kuo, K.H. Wang, Chris Chen, "Pros and cons of different Nitrogen Removal Unit (NRU) technology" Journal of Natural Gas Science and Engineering (2012), Available: www.elsevier.com/locate/jngse.

[2] R. Kevin, Y. Wood, A. Liu, Yueying Yu, "Design, Simulation, and Optimization of Adsorptive and Chromatographic Separations: A Hands-On Approach" First Edition, Published by Wiley-VCH Verlag GmbH & Co. KGaA, 2018.

[3] J.M. Campbell, "Gas conditioning and processing, in: 2: the Equipment and Modules", ninth ed., Campbell Petroleum Series, Oklahoma, 2014.

[4] K.S. Hwang, J.H. Jun, W.K. Lee, "Fixed-bed adsorption for bulk component system non-equilibrium, non-isothermal and non-adiabatic model", Chem. Eng. Sci. 50 (5): 813–825, 1995.

[5] R.T. Yang, "Gas separation by Adsorption Processes", Butterworth, Boston, 1987.

[6] M. Gholami, M.R. Talaie, S. Roodpeyma, "Mathematical modeling of gas dehydration using adsorption process", Chem. Eng. Sci. 65 (22): 5942–5949, 2010.

[7] Ambrosio, "Natural Gas Performance Analysis by Adsorption in Molecular Sieves", Master's Dissertation, Rio de Janeiro, Brazil, 2014.

[8] DM. Ruthven, "Principles of adsorption & adsorption processes", John Wiley & Sons Inc., 1984. ISBN 978-0-471-86606-0.